PROCEEDINGS OF THE ROYAL SOCIETY B

rspb.royalsocietypublishing.org

Research

Cite this article: Andrada E, Rode C, Sutedja Y, Nyakatura JA, Blickhan R. 2014 Trunk orientation causes asymmetries in leg function in small bird terrestrial locomotion. *Proc. R. Soc. B* **281**: 20141405.
http://dx.doi.org/10.1098/rspb.2014.1405

Received: 8 June 2014
Accepted: 7 October 2014

Subject Areas:
biomechanics, physiology, theoretical biology

Keywords:
avian locomotion, pronograde locomotion, biomechanics, stability, leg function

Author for correspondence:
Emanuel Andrada
e-mail: emanuel.andrada@uni-jena.de

Electronic supplementary material is available at http://dx.doi.org/10.1098/rspb.2014.1405 or via http://rspb.royalsocietypublishing.org.

Royal Society Publishing

Trunk orientation causes asymmetries in leg function in small bird terrestrial locomotion

Emanuel Andrada[1], Christian Rode[1], Yefta Sutedja[1], John A. Nyakatura[2,3] and Reinhard Blickhan[1]

[1]Science of Motion, Friedrich-Schiller University Jena, Seidelstraße 20, 07749 Jena, Germany
[2]Institut für Spezielle Zoologie und Evolutionsbiologie mit Phyletischem Museum, Friedrich-Schiller-Universität, 07743 Jena, Germany
[3]Image Knowledge Gestaltung: an interdisciplinary laboratory and Institute of Biology, Humboldt-University, Philippstraße 13, 11015 Berlin, Germany

In contrast to the upright trunk in humans, trunk orientation in most birds is almost horizontal (pronograde). It is conceivable that the orientation of the heavy trunk strongly influences the dynamics of bipedal terrestrial locomotion. Here, we analyse for the first time the effects of a pronograde trunk orientation on leg function and stability during bipedal locomotion. For this, we first inferred the leg function and trunk control strategy applied by a generalized small bird during terrestrial locomotion by analysing synchronously recorded kinematic (three-dimensional X-ray videography) and kinetic (three-dimensional force measurement) quail locomotion data. Then, by simulating quail gaits using a simplistic bioinspired numerical model which made use of parameters obtained in *in vivo* experiments with real quail, we show that the observed asymmetric leg function (left-skewed ground reaction force and longer leg at touchdown than at lift-off) is necessary for pronograde steady-state locomotion. In addition, steady-state locomotion becomes stable for specific morphological parameters. For quail-like parameters, the most common stable solution is grounded running, a gait preferred by quail and most of the other small birds. We hypothesize that stability of bipedal locomotion is a functional demand that, depending on trunk orientation and centre of mass location, constrains basic hind limb morphology and function, such as leg length, leg stiffness and leg damping.

1. Introduction

Our understanding of small avian bipedalism has advanced in recent years. Typically, small birds walk at low speeds and run at high speeds with strongly bent legs and without encompassing aerial phases [1–9]. Compliant gaits such as these are energetically not only costly [10], but also offer advantages in return. Long stride lengths and contact times [10–12] permit high-speed locomotion with relatively low peak loading forces, which exceed body weight only slightly [8,10,13]. It has been shown recently that quail fix the angle between their legs before touchdown [8]. By combining experimental data with simulations carried out using the bipedal spring-loaded inverted pendulum (SLIP) [14,15] model, Andrada *et al.* [8] showed that this leg alignment diminishes local instability and increases tolerance of changes in ground level. However, although our understanding of avian bipedal locomotion has improved in recent years, some features, such as the dynamic role of the trunk and its interaction with the legs, remain largely unexplored [16].

The global dynamics of avian bipedalism can be approximated using the SLIP model [9,17]. However, in contrast to the symmetric ground reaction force (GRF) produced in SLIP simulations of bouncing gaits, the GRF exerted by birds appears to be left-skewed [9,17–20] and was found to be more vertically oriented [9] than the virtual leg, assumed to act between the centre of mass (CoM) and the centre of pressure (CoP). The SLIP model can address neither the question of how such

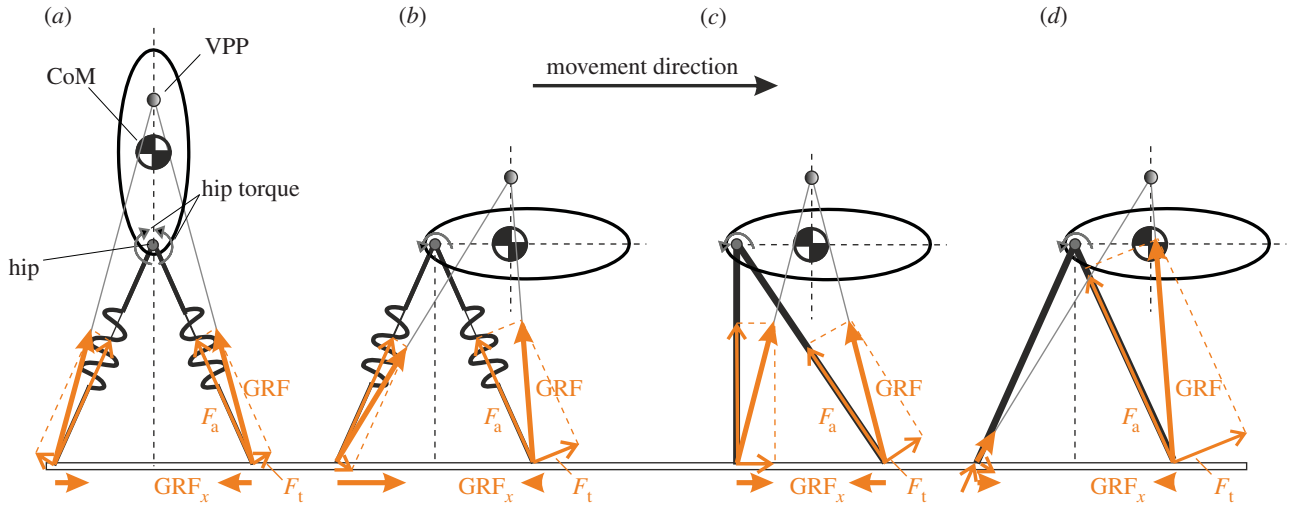

Figure 1. Trunk posture, virtual pivot point (VPP) control and leg function. VPP control orients the ground reaction forces (GRFs) to a point above the centre of mass (COM) in order to balance the trunk. The hip torque generates a tangential force (F_t) which in combination with the axial force (F_a) redirects the GRF to the VPP. The arrow marks the direction of movement in all examples. (*a*) If the VPP point and the CoM are located vertically above the pelvis, symmetric axial effective leg function (e.g. spring-like) can produce steady-state locomotion because braking and accelerating forces (GRF_x) cancel each other out. (*b*) When the trunk is pitched forwards, symmetric axial effective leg function produces acceleration. (*c*,*d*) Asymmetric effective leg behaviour may permit steady-state locomotion with a pronograde trunk. (*c*) Pure kinematic asymmetry: forces are symmetric with respect to the CoM and accelerative and braking forces compensate each other. (*d*) Pure kinetic asymmetry: large forces in the short early stance phase are compensated by smaller forces in the remainder of stance phase. (Online version in colour.)

forces may evolve in the bouncing gaits of birds nor how the problem of balancing the trunk is solved.

By replacing the point mass of the SLIP model with a trunk, Maus *et al*. [21] showed that humans stabilize their trunk when walking by directing the GRF above the CoM. In human walking and chicken running, the GRF roughly intersects at a point above the CoM [21], a finding consistent with more vertically aligned GRF in quail, which may also have benefits in reducing energy consumption during running [22]. Maus *et al.* [21] termed this intersection point the virtual pivot point (VPP). By setting the GRF to intersect the VPP, they were able to calculate hip torques in their simulations of human walking and found that these hip torques led to stabilization of the upright trunk.

However, in contrast to the upright trunk found in humans, the trunk orientation of most birds is almost pronograde, leading to their CoM being located not above the pelvis but further cranially. This imposes constraints on the effective leg (between hip and CoP) function during locomotion, which are likely to be independent of the variations in segmental hindlimb morphology observed in relation to differences in ecology and biomechanical demands. For example, a CoM that is shifted cranially requires increased hip extension torques to balance the trunk against gravity. It has been shown in small and medium-sized birds that hip extension torques occur throughout stance [9,17,23]. In combination with spring-like leg operation along the leg axis, these hip extension torques introduce a tangential force at the tip of the leg, which results in forward acceleration of the CoM (figure 1*b*). To achieve locomotion at a steady speed, two effective leg strategies can be exploited. The first is a kinematic asymmetry with respect to the hip, which achieves symmetry of foot contact with respect to the CoM (i.e. longer effective legs at touchdown and shorter effective legs at lift-off; figure 1*c*). The second is a kinetic asymmetry effected by the exertion of higher forces in the early stance phase and lower forces in the remaining stance phase. This results in a GRF pattern that is skewed to the left (figure 1*d*). At the same time, the angular momentum about the CoM produced during each stride must be zero to achieve trunk balance. On the basis of these considerations, our main hypothesis is that asymmetric leg behaviour during avian bipedalism, as reflected in the skewed GRF profile and touchdown–lift-off asymmetry, is a result of the pronograde trunk posture and the factor that permits steady-state locomotion.

Our goal was to highlight the dynamic effects of a pronograde trunk on leg function and stability during locomotion. In order to do so, we first verified the existence of a VPP in quail terrestrial locomotion by analysing synchronously recorded kinematic and kinetic quail locomotion data. We then analysed numerically the interrelatedness of trunk pitch and leg function during locomotion using parameters obtained during experiments in forward simulations of a minimalistic pronograde VPP (PVPP; figure 2*b*) quail model. This allowed us to elucidate whether asymmetric leg behaviour in small bird locomotion is a corollary of pronograde trunk orientation.

2. Material and methods

(a) Experimental data

For the purposes of this study, we re-analysed the dataset used by Andrada *et al*. [9], focusing, however, on different aspects. The materials and methods used to obtain kinematic data, the position of the CoM, GRFs and %congruity were documented in detail in the original paper and are only summarized here briefly.

Eight adult common quails (Phasianidae: *Coturnix coturnix*, Bonnaterre 1791) weighing between 180 and 247 g moved across a walking-track 3 m long at their preferred speeds. Kinematics and GRFs were recorded simultaneously. For the kinematic analysis, synchronized, biplanar X-ray videography (Neurostar, Siemens, Erlangen, Germany) data were used. X-ray recordings were taken from the lateral and ventral projections. The X-ray machine operated at 40 kV and 53 mA, with a sampling frequency of 1 kHz. We measured three-dimensional GRFs and CoP using two custom-built (8×9 cm) force plates integrated into the walking-track. GRFs were collected at 1 kHz and force, and X-ray

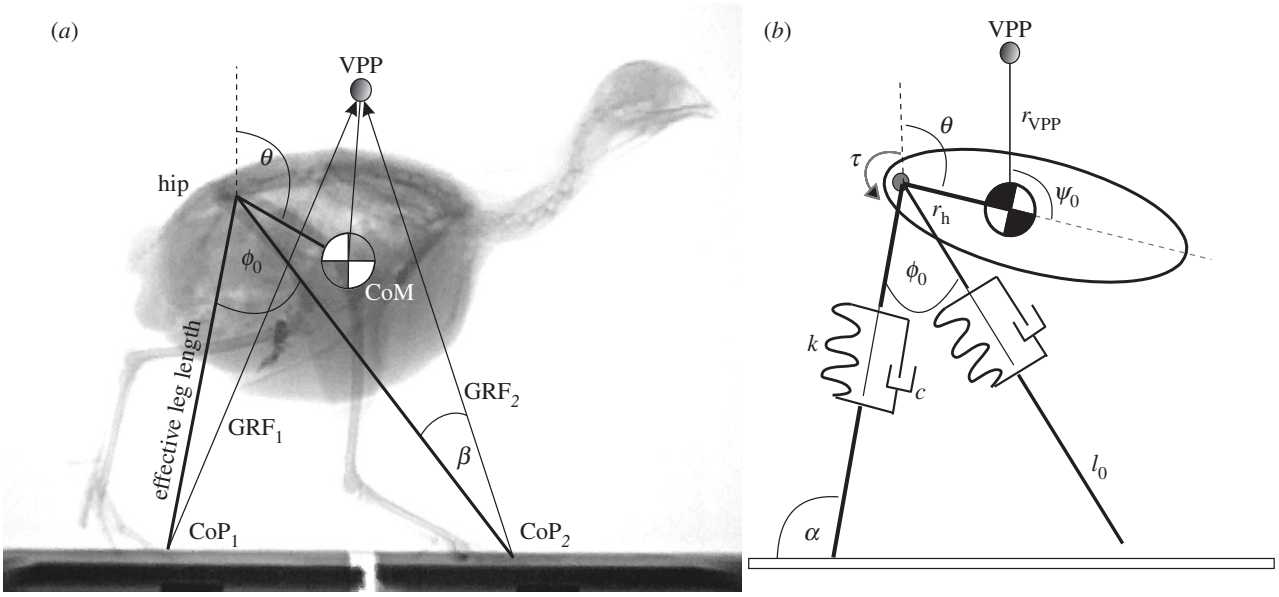

Figure 2. Quail and model. (*a*) Lateral X-ray projection of a quail traversing the two force plates custom-built to obtain single limb kinetic data. Schematic drawing superimposed onto X-ray still image depicting VPP, GRFs, effective legs at touchdown (segments hip–CoP1, hip–CoP2), aperture angle at touchdown ϕ_0, trunk angle θ and angle between effective leg and GRF β. (*b*) Minimalistic quail model using a VPP for postural control, and asymmetric leg behaviour modelled as parallel spring and damper. τ, hip torque; ψ_0, angle between trunk and VPP; α, angle between ground and effective leg; k, leg stiffness; c, leg damping; l_0, rest length at touchdown; r_h, distance hip–CoM; r_{VPP}, distance CoM–VPP.

data synchronized electronically (post-trigger; see the electronic supplementary material for further information).

As described in references [7,9], we calculated the instantaneous position of the body's CoM from kinematic and cadaveric data. For the purposes of this study, trials were categorized into walking, grounded running or running. We used the percentage of congruity [24] between the CoM's potential and kinetic energy to discriminate bouncing gaits (grounded running and running) from vaulting gaits (walking). Grounded running deviates from running in featuring double contact phases and no aerial phases.

To determine the VPP, the vertical and horizontal distances between CoM and CoP were measured, and the scaled GRF from 0.1 to 0.9 of stance then drawn into a CoM-fixed coordinate system (figure 3*d*). VPP height is defined as the vertical distance from the CoM at which the horizontal spread between the GRFs is minimal. To determine axial leg function, the sagittal plane GRF of each leg was projected onto the effective leg axis connecting the hip and the respective CoP. Because of the asymmetric leg behaviour we observed in the results, we modelled axial leg function as parallel spring and damper elements,

$$F_a = k(l_0 - l) - c\dot{l}. \tag{2.1}$$

F_a is the axial leg force, l_0 is the rest length of the spring, l is the instantaneous effective leg length, i is the rate of change in the effective leg length, k is the effective leg stiffness and c is the effective leg damping. We obtained k and c with a non-linear fit by minimizing for each trial the sum of squared distances between measured forces and the forces calculated with equation (2.1) (using effective leg length data from experiments). We obtained a measure for the quality of the fit by dividing the sum of the residuals by the number of data points and the maximal leg force.

We defined the angle ϕ_0 between legs at touchdown as the angle between CoP1–hip–CoP2 (figure 2*a*), and mean trunk orientation θ_{mean} as the mean angle between the vertical and the vector hip–CoM measured clockwise (figure 2*a*) over one step.

We were able to obtain for final data analysis a total of 86 steady-state strides (32 walking, 46 grounded running and 8 running) captured using biplanar X-ray recording and synchronous, single limb GRF traces. We used the *t*-test in SPSS 18 (IBM, Armonk, NY) to determine whether template-related parameters are gait-related (significance level $p < 0.05$).

(b) Simulations

The sagittal plane PVPP model consists of a rigid body of mass m with a moment of inertia J connected at the hip to two massless legs modelled as parallel spring-damper elements (figure 2*b*). The trunk can pivot freely about the hip axis. The CoM of the model is located at a distance r_h from the hip at an inclination θ from the vertical (figure 2*b*). The location of the VPP is given by the distance r_{VPP} from the CoM and the inclination ψ_0 from the body axis (figure 2*b*). The equations of motion are $m\ddot{x} = F_x$, $m\ddot{y} = -mg + F_y$ and $J\ddot{\theta} = r_{VPP}(F_x \cos(\theta - \psi_0) - F_y \sin(\theta - \psi_0))$, where F_x and F_y are the sum of the horizontal and vertical components of the GRF of the legs, g is gravitational acceleration, and $\ddot{x}$,$\ddot{y}$ and $\ddot{\theta}$ are, respectively, the CoM horizontal, CoM vertical and trunk angular accelerations. The following constant model parameters were taken from literature ($r_h = 0.035$ m [9]) and our experimental results: $l_0 = 0.12$ m, $m = 0.2$ kg; $J = 1330 \times 10^{-7}$ kg m^2 (trunk, neck and head modelled as a cylinder). We formed two gait categories of initial parameters based on the parameters obtained from quail walking and bouncing gaits: (i) walking-like, with $k = 75$ N m^{-1}, $\phi_0 = 45^\circ$ and horizontal initial speed $v_{x0} = 0.4$ m s^{-1}, and (ii) bouncing-like, with $k = 100$ N m^{-1}, $\phi_0 = 50^\circ$ and $v_{x0} = 0.6$ m s^{-1}. We based this classification on the significant differences observed for these parameters between grounded running and walking (table 1). Just as in experiments, we relied on %congruity to discriminate walking from bouncing, and then distinguished running from grounded running by checking for flight phases. A rigorous analysis of stability was not the aim of this paper. In accordance with literature [25], we defined stability as the ability to cope with even undetected perturbations (see the electronic supplementary material for further explanations about the model and stability). To exemplarily show robustness, we applied a step-down step-up perturbation of 0.3 l_0 and a step-down

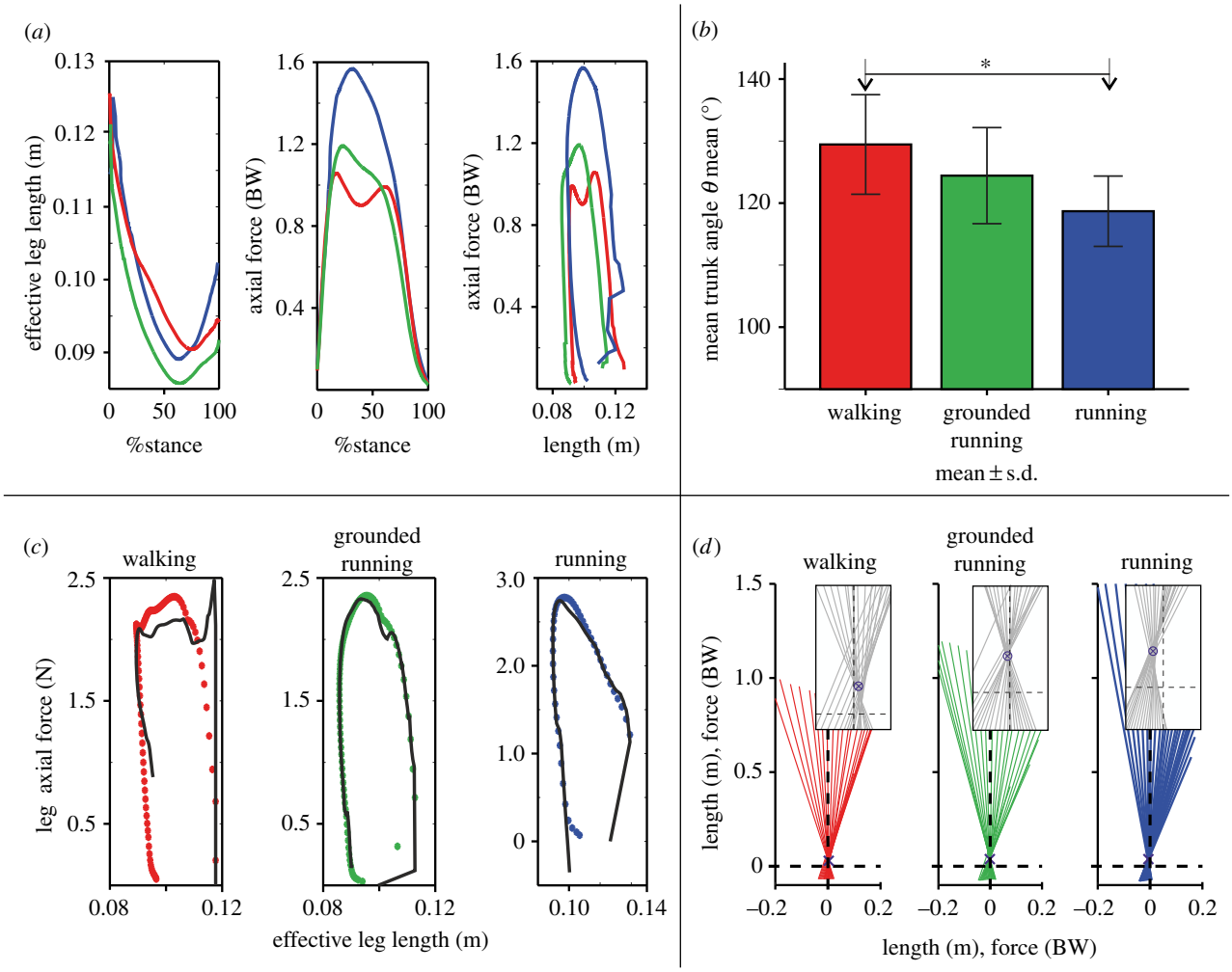

Figure 3. Variation of model-relevant parameters during locomotion of the quail. (*a*) Effective leg length, axial force in the effective leg and axial leg function (axial force over leg length) in walking (red), grounded running (green) and running (blue), respectively. Curves are mean values (table 1). (*b*) Mean and standard deviation of trunk angle during walking, grounded running and running. The asterisk highlights the significant difference between walking and running ($p = 0.006$). (*c*) Examples of axial leg function in the quail during walking, grounded running and running (coloured asterisks), and results of the nonlinear fit using a parallel spring-damper model (solid lines). (*d*) GRF traces in the sagittal plane. An estimated virtual pivot point (VPP) relative to the CoM is displayed during walking (VPP height = 0.029 m), grounded running (VPP height = 0.038 m) and running (VPP height = 0.037 m). (Online version in colour.)

Table 1. Gait-related effective leg parameters and VPP height obtained from experimental data. *k*, leg stiffness from fit; *c*, leg damping from fit; l_0, leg length at touchdown; ϕ_0, aperture angle between legs; r_{VPP}, distance VPP–CoM (mean ± 1 s.d.); *p*, significance *t*-test < 0.05. w, walking; gr, grounded running; r, running.

parameter	walking	*n*	grounded running	*n*	running	*n*	*p* w versus gr	*p* w versus r	*p* gr versus r
k (N m^{-1})	76.4 ± 40.9	28	106.2 ± 43.8	44	102.8 ± 22	8	0.016	0.05	n.s.
c (Ns m^{-1})	6.4 ± 3.7	28	6.0 ± 2.1	44	3.8 ± 1.1	8	n.s.	0.002	<0.01
l_0 (m)	0.125 ± 0.01	24	0.122 ± 0.03	36	0.114 ± 0.01	8	n.s.	n.s.	0.04
ϕ_0 (°)	43.5 ± 4.3	18	48 ± 4.7	21	not defined		<0.001	—	—
r_{VPP} (m)	0.043 ± 0.024	28	0.054 ± 0.024	32	0.051 ± 0.025	8	0.041	n.s.	n.s.

perturbation of 0.1 l_0 after 100 steps and let the simulation continue for another 100 complete steps.

3. Results

(a) Experimental data

Quail walked at speeds ranging from 0.15 to 0.51 m s^{-1} (mean 0.34 m s^{-1}), used grounded running at speeds between 0.42 and 0.79 m s^{-1} (mean 0.58 m s^{-1}) and ran with an occurrence of an aerial phase at speeds ranging from 0.75 to 1.56 m s^{-1} (mean 1.06 m s^{-1}).

The birds exhibited a VPP in all gaits (figure 3*d*), and its position relative to the CoM varied significantly only between walking and grounded running (mean of VPP height r_{VPP}: walking 0.043 m, grounded running 0.056 m, running 0.051 m; table 1). The mean trunk angle θ_{mean} decreased from walking through grounded running to

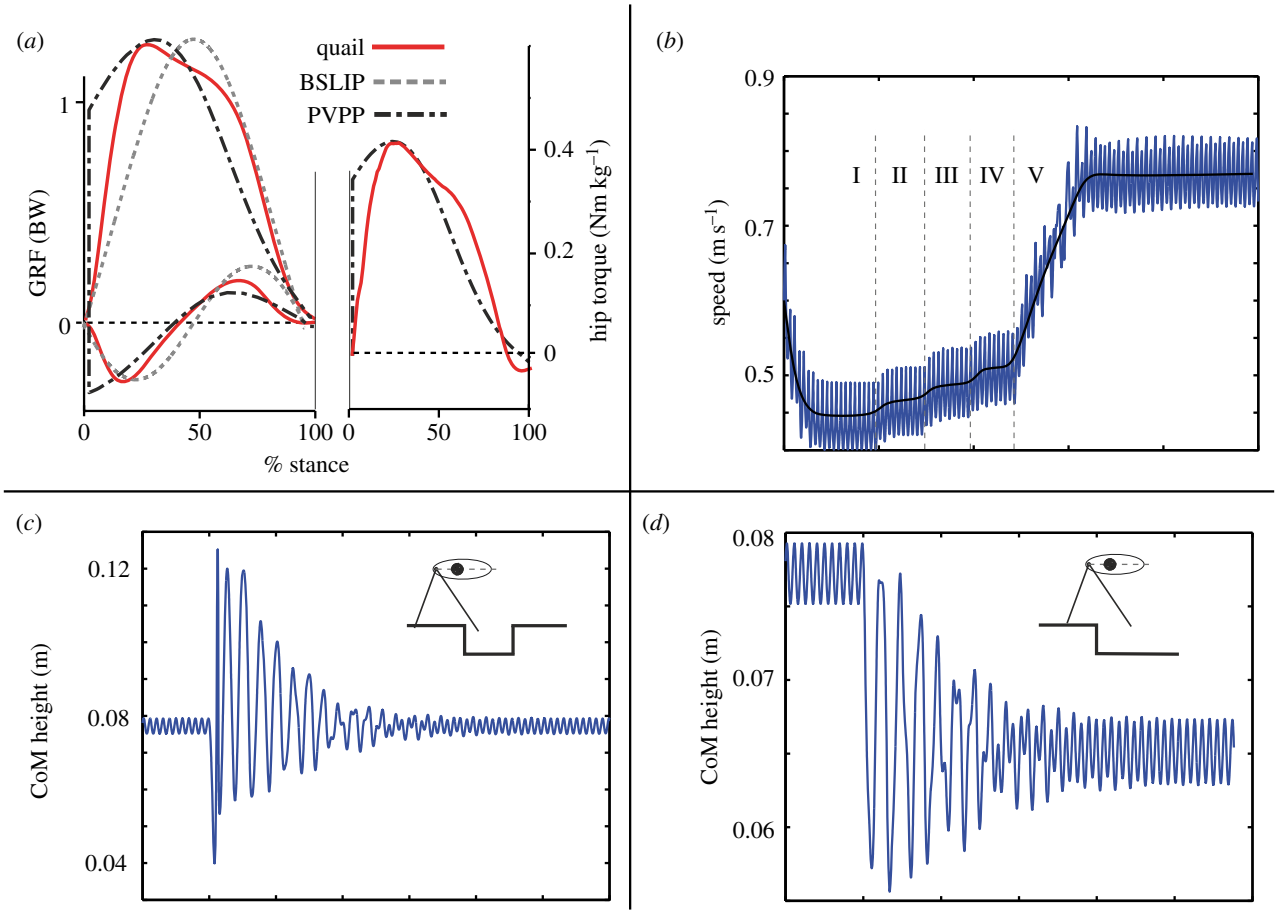

Figure 4. Ground reaction forces (GRFs), hip torque, speed regulation and robustness of the pronograde VPP model (PVPP). (*a*) Experimental versus model GRF and hip torque during grounded running. Note that the GRFs obtained using the PVPP model are left-skewed owing to the action of the damper (experimental and SLIP curve data taken from Andrada *et al.*). (*b*) Speed regulation in the PVPP model: starting from a speed of 0.6 m s^{-1}, model speed can be regulated in the stable regions just by changing damping constant ($I_c = 5.8$, $II_c = 5.5$, $III_c = 5.2$, $IV_c = 5.0$, $V_c = 4.2$ Ns m^{-1}). (*c*,*d*) Robustness of the PVPP model to perturbations in ground level. (*c*) CoM traces before, during and after a step-down step-up perturbation of 30% of leg length. Note that the model returns to the same trajectory after a few steps. (*d*) CoM traces before, during and after a step-down perturbation of 10% of leg length. After the perturbation, the model stabilizes in a different periodic motion. Model parameters for all subplots are $k = 100$ N m^{-1}, $c = 4.2$ Ns m^{-1}, $\phi_0 = 50°$, $r_{VPP} = 0.04$ m, $\psi_0 = 131.8°$. (Online version in colour.)

running (figure 3*b*), and differed significantly between walking and running.

The angle between legs at touchdown (TD; figure 2*a*) differed significantly between walking (mean $\phi_0 = 43.5°$) and grounded running (mean $\phi_0 = 48°$; table 1). Effective leg length at TD varied significantly only between grounded running and running (table 1). Effective leg length displayed strong asymmetry during the contact phase (longer legs at TD and shorter legs at toe-off; figure 3*a*).

The parallel spring-damper system fitted walking data less well than grounded running and running data (figure 3*c*). The average deviation of model force from measured force was 0.14 (walking), 0.08 (grounded running) and 0.04 (running) of the maximal force. Mean effective leg stiffness was similar during grounded running and running, and in both cases higher than during walking (table 1). The mean value of the effective leg-damping constant c was highest during walking, decreased slightly during grounded running and was significantly lower during running (table 1).

(b) Simulations

We simulated quail locomotion using a minimalistic PVVP model (see Material and methods). Without damping, speed constantly increased during simulations as a result of the mechanism explained in figure 1*b*. In all gaits, stable locomotion (i.e. after perturbations, even undetected, the model converged asymptotically to a periodic gait) was found only for trunk orientations exceeding 107°, a value similar to the trunk inclinations observed in experiments (figure 3*b*). GRFs in stable simulations were left-skewed (e.g. grounded running, figure 4*a*, left). Hip torques in simulations were similar to those observed in experiments (e.g. grounded running, figure 4*a*, right). Without parameter optimization, PVPP locomotion was robust in response to perturbations in ground level up to 0.3 l_0 (figure 4*c*,*d*). The results presented below are stable simulations, with damping values and trunk inclinations based on experimental data obtained from live quail.

(c) Simulations using walking-like parameters

Using parameters obtained from walking quail (effective leg stiffness and damping, average speed of locomotion; see Material and methods and table 1), simulations yielded walking speeds ranging from 0.17 to 0.65 m s^{-1} and grounded running speeds ranging from 0.2 to 1.2 m s^{-1}. Intriguingly, the majority of the self-stable solutions found were grounded runs (78%; figure 5*a*), followed by walking (22%; figure 5*a*).

The walking domain is tetrahedral in shape and located in the upper parameter range. Trunk angles become steeper almost linearly as VPP height and damping decrease. No stable walking solutions were found for VPP height less than

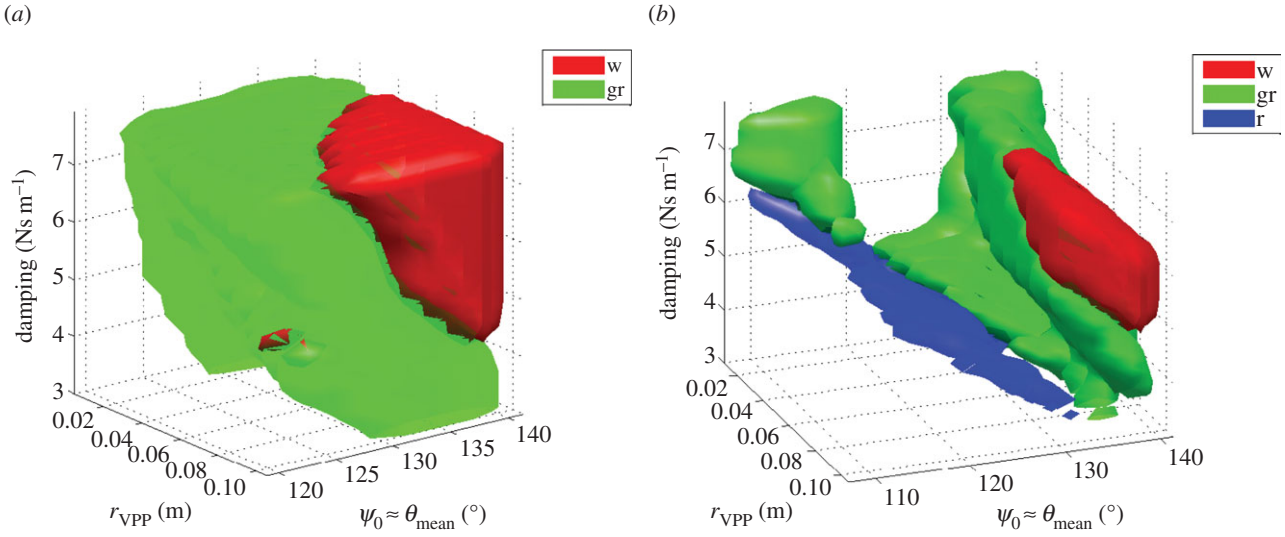

Figure 5. Fields of stable locomotion for (*a*) walking-like and (*b*) bouncing-like parameters (see Material and methods). The majority of the stable solutions obtained correspond to grounded running (gr). Note that running (r) exists at smaller trunk angles (less inclined from the vertical) and lower damping values than grounded running and walking (w) (right). Higher stiffness and lower damping values facilitate aerial phases and more symmetric locomotion. The opposite applies to walking. (Online version in colour.)

0.04 m or damping lower than 4 Ns m^{-1}. Grounded running solutions surround the walking domain, exist at all investigated VPP heights and start at trunk angles close to 120°.

(d) Simulations using bouncing-like parameters

Using parameters obtained from bouncing-like quail gaits (see Material and methods and table 1), simulated walking speeds ranged from 0.36 to 0.54 m s^{-1}, grounded running speeds ranged from 0.2 to 1.7 m s^{-1}, and aerial phase running speeds ranged from 0.52 to 1.85 m s^{-1}. Again, most of the stable solutions were grounded running (80%, figure 5*b*, green). Walking (figure 5*b*, red) and aerial phase running (figure 5*b*, blue) made up the remaining 20% in equal measure.

Grounded running existed in two separate volumes: a small one located at damping values exceeding 5.5 Ns m^{-1} with relatively shallow trunk angles between 107° and 119° and VPP heights between 0.01 and 0.04 m, and a large one located at VPP heights higher than 0.01 m and mean trunk angles exceeding 120°. For VPP heights higher than 0.06 m, damping greater than 5 Ns m^{-1} and mean trunk angles exceeding 130°, simulations indicated stable walking. The two grounded running domains were connected by a long, thin, inclined volume of running solutions that stretched from mean trunk angles of 110° at relatively high damping values (6.2 Ns m^{-1}) to mean trunk angles close to 135° at damping values close to 3.2 Ns m^{-1}, and comprised almost the whole range of VPP heights.

4. Discussion

The aim of this study was to analyse the dynamic consequences for leg function during locomotion while balancing a pronograde trunk. We postulated that asymmetric (with respect to the hip) leg function is a prerequisite for the pronograde trunk orientation observed during avian steady-state locomotion. Quail use a combination of the predicted asymmetries (figure 1*c*,*d*). By simulating quail gaits using the minimalistic PVPP model in conjunction with parameters obtained through experiments with live quail, we were able to show that asymmetric leg function facilitates steady-state locomotion. Surprisingly, we found not only pronograde walking, but aerial phase running and large ranges of grounded running to be both stable and robust, which could provide a strong biomechanical rationale for why the latter gait seems to be so significant in quail, and perhaps birds in general.

On the basis of a VPP reported in running chicken and walking humans [21], we presumed that the more vertical GRF vector observed by Andrada *et al.* [9] during quail locomotion could indicate movement strategies resulting in a VPP. This indeed turned out to be the case, and we found that quail display a VPP in all investigated gaits.

Our parameter fit revealed lower effective stiffness in walking than in grounded running and running (table 1). In contrast, damping was highest during walking (table 1), leading to more asymmetric kinematic leg function (figure 3*a*), and therefore to earlier foot lift-off. This observation ties in with previously published results on leg retraction during stance, according to which amplitude is lower when birds move more slowly [1,2,6,26–28]. On the other hand, the swing phase, characterized by the swing time and the angle of attack is largely independent of speed in the species of bird investigated [1,6,7,26]. This suggests that birds regulate speed during stance, increasing stride length by reducing leg damping, which leads to more symmetrical, spring-like leg motion, and simultaneously decreasing contact times [1,6,8,28] by increasing leg stiffness (figure 3*a* and table 1).

How can such effective leg behaviour be achieved physiologically? Investigations in human subjects demonstrate that, in the case of ankle extensors, increasing the speed of contraction reduces force development [29]. Switching to running causes the same muscles to operate closer to isometric action, whereas the displacement is covered by the elasticity of the tendons. This same mechanism has been observed in running turkeys [30] and might also apply to quail switching from walking or grounded running to aerial phase running, where the leg undergoes a more pronounced stretch–shortening cycle than in running (figure 3*a*). This shift from a behaviour dominated by muscle properties to a behaviour increasingly dominated by elastic tissues, as documented in humans and turkeys [29,30], may explain the shift we observed in the viscoelastic properties of the quail leg.

Simple mechanical models (referred to by Full & Koditschek [31] as templates) have been very useful in helping us to understand basic features of locomotion. On the other hand, they are limited in their capacity to explain more detailed field observations because of a lack of parameter space. The nonlinear axial leg function and left-skewed GRF profiles obtained in recent studies [9,32], for example, have highlighted the need for a stepwise refinement of the SLIP template. This study features an expansion of the bipedal SLIP model. Despite its relative simplicity, our PVPP model incorporates three key features of bird locomotion: (i) the pronograde trunk, (ii) asymmetric compliant leg behaviour along the leg axis (modelled as a parallel spring-damper system), and (iii) a fixed aperture angle as a leg alignment strategy. All three features were inferred from *in vivo* experiments involving quail.

In PVPP simulations, the VPP will always tend to be above the CoM. This is because if the VPP position deviates from vertical above the CoM, restoring hip torques increase. This mechanism allows the mean orientation of the trunk to be set by positioning the VPP relative to it. The more cranial the VPP, the less inclined the mean orientation of the trunk. The more dorsal the VPP, the more inclined the mean orientation of the trunk. In the special case where the orientation of the trunk is vertical (hip, CoM and VPP aligned), symmetric effective leg behaviour along the leg axis (spring-like) generates via VPP the torque pattern necessary to stabilize locomotion [21]. However, as the trunk is pitched, the CoM and VPP are translated cranially with respect to the hip. Although trunk stability might be achieved, the model will increase speed constantly when spring-like legs are involved as the accelerative forces become larger than the braking forces (figure 1). Non-accelerative pronograde locomotion, then, requires asymmetric leg function, in our case modelled by a parallel damper element.

Our findings offer an explanation for the characteristic GRF profile observed in bird locomotion, whose skew to the left highlights an adjustment in leg function to the needs of trunk posture: the leg has to dissipate energy in order to avoid the acceleration of the CoM (figures 1 and 3*a*,*c*). In our model, the damper left-skews the GRF profile by increasing leg forces after touchdown. During leg extension, the damper decreases leg forces and leads to early lift-off, inducing at the same time a kinematic asymmetry. Effective leg behaviour such as this may be produced in birds by the damping properties of muscles [33,34].

At the limb joint level, quail seem to employ a division of work principle. While the most proximal joints retract and protract the limb actively, the intertarsal joint acts as a spring, and the tarsometatarso-phalangeal joint, which engages in negative work loops, may function as a damper [9]. This division of work is represented in the PVPP model by the hip torques that introduce energy, the axial spring and the axial damper. Earlier studies in running guinea fowl have also found that more distal joints are likely to act as springs, whereas more proximal ones (hip, knee) contribute to propulsion in both level running and unexpected drops [17,23]. The same division of work seems to apply to small mammals, too [35–37]. The crouched leg posture of smaller animals in general leads to more intrinsic muscle-related damping, greater relative muscle mass and less effective biological springs [38].

One of the most important findings of the present work is that stable pronograde locomotion exists for quail mass dimensions only at the mean trunk inclinations observed in experiments involving actual quail locomotion (greater than 107°). Note that all relevant model parameters (leg length at touchdown, inertia, stiffness, damping, aperture angle, hip–CoM distance and VPP height) were obtained from experimental data pertaining to living quails. Intriguingly, the majority of stable solutions are grounded runs. Recent studies have argued that limb morphology, especially in small-to-medium-sized avian species, maximizes the potential advantages of grounded running [6–13,30,39,40]. Our simulations, which reveal stability for this gait, add a functional argument for the occurrence of grounded running. In addition, our results suggest that, given the general morphology of birds (i.e. crouched hind limbs, nearly pronograde trunk orientation), specific geometric relationships between effective leg length at touchdown, the position of the CoM with respect to the hip and VPP height are mandatory in order to achieve stable locomotion.

Despite different leg lengths in small birds, they apply a similar angle of attack [1,6,9]. Hence, based on our results, we predict that birds with longer legs will display a more symmetric leg function, because more time is available for decelerating horizontal forces to achieve steady-state locomotion (figure 6). Similarly, a caudal shift of the CoM is expected to lead to a similar effect. Species of bird whose CoM is more cranial with respect to the hip would be expected, for example, to increase the inclination of their trunk so as to reduce the horizontal hip–CoM distance, and/or to display increased effective leg length, either through relatively long phalanges or the use of larger angles. Digit lengths in avian feet have been shown not to correlate clearly with either ecology or phylogenetic position [41]. Our results suggest that the relative position of the CoM imposes a functional constraint on the length of the phalanges and may thus help to explain the surprising result obtained by Stoessel *et al.* [41].

Trunk orientation and leg function are coupled. In humans, the placement of the hip below the CoM allows a more elastic operation of the leg (figure 1*a*), leading to less expected kinetic and kinematic asymmetry, and to hip extension and flexion torques. Still, both asymmetries are present, but their source is different from quail. In human, the leg is about 5% longer at take-off compared with touchdown [42,43], whereas in quail the leg is 25% shorter at take-off (figure 3*a*). In humans, this kinematic asymmetry seemingly results from elastic ankle function [44]. The kinetic asymmetry observed in human running is mostly explained by the impact forces at TD [45,46]. In contrast, in quail, the impact is much lower owing to the absence of flight phases, the low mass of the highly compliant avian foot and the aperture angle [8,9]. Our results indicate that an inclined trunk necessitates damping in the leg, which is the source of the kinetic and the kinematic asymmetry.

Stability during locomotion has mostly been analysed for tractability using templates such as the SLIP model [14,15] for running and the bipedal SLIP model for walking [47]. Both conservative models can exhibit periodic motion that is only partially asymptotically stable (i.e. it cannot stabilize changes in system energy). However, animals are not energy conserving, so recent investigations have centred on modified spring-mass models capable of energy management [48,49]. Commonly, leg properties such as effective leg stiffness or effective leg length are adapted during stance. A different approach is to add hip torque [50], resulting in a non-physical SLIP model. Most of these approaches are based on the way humans [42,51–53] and birds [17,54,55] seem to adapt stiffness, leg retraction and leg length in advance of or in response to a perturbation. However, even without optimizing parameters, our model is able to cope with ground-level perturbations

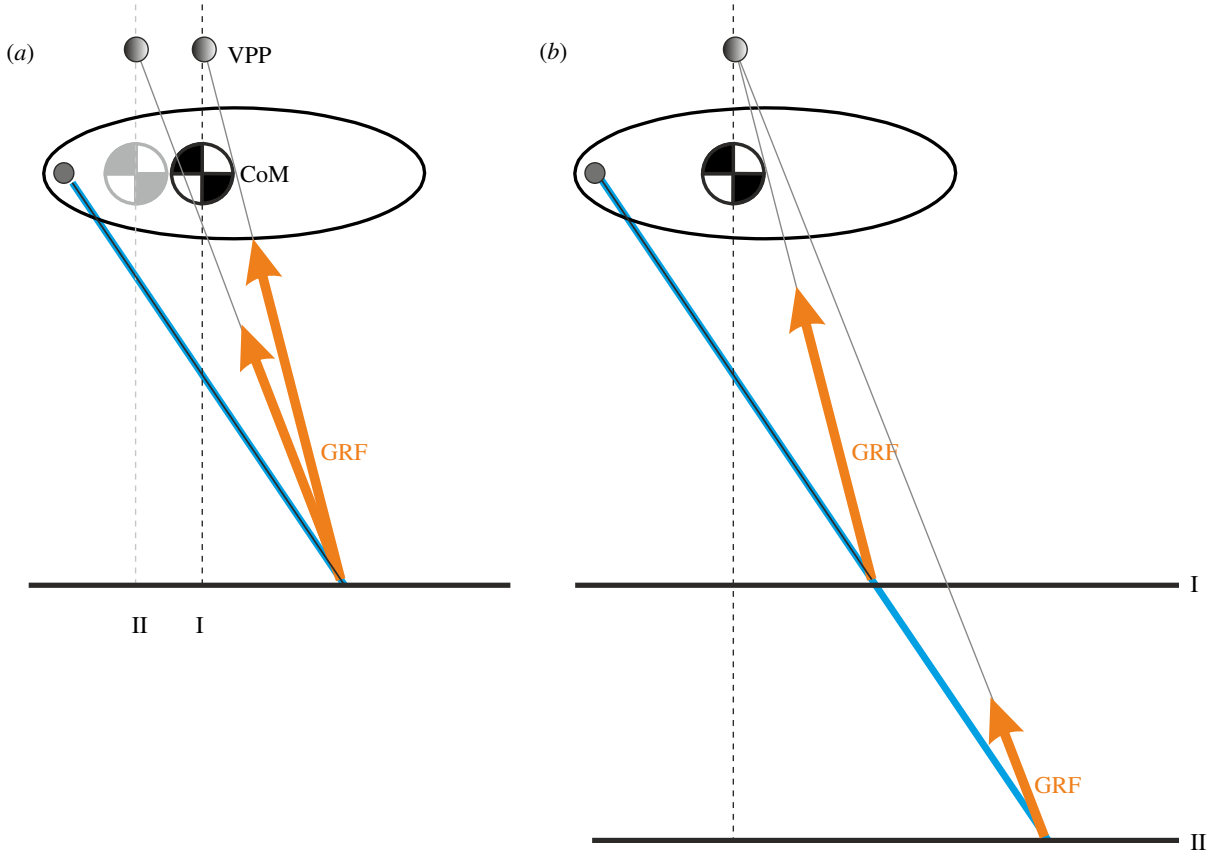

Figure 6. Two ways of reducing asymmetric leg function. (*a*) A caudal shift of the CoM. (*b*) Longer legs, and hence more protracting strides. Assuming constant horizontal velocity, both alternatives lead to more available time to develop decelerating horizontal forces necessary to achieve steady-state locomotion. As a result, the GRF rise can be less steep. In our model, this would require less damping, which would reduce kinetic and kinematic asymmetry at the same time. (Online version in colour.)

of up to 30% of leg length without requiring either parameter changes or feedback control (figure 4*c*). Moreover, the model is also extremely insensitive to errors in parameters such as aperture angle, effective leg stiffness and damping. This surprising robustness may explain the evolutionarily conservative pronograde orientation of the trunk in combination with the widespread occurrence of grounded running in birds. The model may even yield new insights into the relationship between trunk posture and leg function in theropod dinosaur locomotion. Taking into account, for instance, that the theropod trunk was almost pronograde but that the CoM was more caudal [28,56] than in birds, it is likely that theropod leg function was much more symmetric than in modern quail.

Ethics statement. The Committee for Animal Research of the State of Thuringia, Germany, approved the animal care and all experimental procedures (registry number: 02-47/10).

Acknowledgements. We thank Ben Derwel for his help in computing quail VPP. Rommy Petersohn and Ingrid Weiß helped with X-ray data acquisition. We thank Lucy Cathrow and Brandon Kilbourne for improving the English. Three reviewers' comments helped to improve and clarify the manuscript. E.A. and R.B. conceived the study; E.A. and J.A.N. designed and conducted the experiments; E.A. analysed the experimental data; E.A., C.R. and Y.S. conducted simulations; and E.A. and C.R. drafted the manuscript. All authors contributed to the interpretation of the results and revised the manuscript.

Funding statement. This research was supported by DFG (German Research Council) grant nos. Bl 236/22-1/3 and Fi 410/15-1/3.

References

1. Gatesy SM, Biewener AA. 1991 Bipedal locomotion: effects of speed, size and limb posture in birds and humans. *J. Zool.* **224**, 127–147. (doi:10.1111/j.1469-7998.1991.tb04794.x)
2. Gatesy SM. 1999 Guineafowl hind limb function. I: Cineradiographic analysis and speed effects. *J. Morphol.* **240**, 115–125. (doi:10.1002/(SICI)1097-4687(199905)240:2<115::AID-JMOR3>3.0.CO;2-Y)
3. Reilly SM. 2000 Locomotion in the quail (*Coturnix japonica*): the kinematics of walking and increasing speed. *J. Morphol.* **243**, 173–185. (doi:10.1002/(SICI)1097-4687(200002)243:2<173::AID-JMOR6>3.0.CO;2-E)
4. Abourachid A. 2001 Kinematic parameters of terrestrial locomotion in cursorial (ratites), swimming (ducks), and striding birds (quail and guinea fowl). *Comp. Biochem. Physiol. A, Mol. Integr. Physiol.* **131**, 113–119. (doi:10.1016/S1095-6433(01)00471-8)
5. Nudds RL, Folkow LP, Lees JJ, Tickle PG, Stokkan KA, Codd JR. 2011 Evidence for energy savings from aerial running in the Svalbard rock ptarmigan (*Lagopus muta hyperborea*). *Proc. R. Soc. B* **278**, 2654–2661. (doi:10.1098/rspb.2010.2742)
6. Stoessel A, Fischer MS. 2012 Comparative intralimb coordination in avian bipedal locomotion. *J. Exp. Biol.* **215**, 4055–4069. (doi:10.1242/jeb.070458)
7. Nyakatura JA, Andrada E, Grimm N, Weise H, Fischer MS. 2012 Kinematics and center of mass mechanics during terrestrial locomotion in northern lapwings (*Vanellus vanellus*, Charadriiformes). *J. Exp. Zool. A, Ecol. Genet. Physiol.* **317**, 580–594. (doi:10.1002/jez.1750)
8. Andrada E, Rode C, Blickhan R. 2013 Grounded running in quails: Simulations indicate benefits of observed fixed aperture angle between legs before touch-down. *J. Theor. Biol.* **335**, 97–107. (doi:10.1016/j.jtbi.2013.06.031)
9. Andrada E, Nyakatura JA, Bergmann F, Blickhan R. 2013 Adjustments of global and local hindlimb properties during terrestrial locomotion of the

common quail (*Coturnix coturnix*). *J. Exp. Biol.* **216**, 3906–3916. (doi:10.1242/jeb.085399)

10. McMahon TA, Valiant G, Frederick EC. 1987 Groucho running. *J. Appl. Physiol.* **62**, 2326–2337.
11. Schmitt D. 1999 Compliant walking in primates. *J. Zool.* **248**, 149–160. (doi:10.1111/j.1469-7998.1999.tb01191.x)
12. Daley MA, Usherwood JR. 2010 Two explanations for the compliant running paradox: reduced work of bouncing viscera and increased stability in uneven terrain. *Biol. Lett.* **6**, 418–421. (doi:10.1098/rsbl.2010.0175)
13. Andrada E, Nyakatura JA, Müller R, Rode C, Blickhan R. 2012 Grounded running: an overlooked strategy for robots. In *Autonomous mobile systems 2012* (eds P Levi, O Zweigle, K Häußermann, B Eckstein), pp. 79–87. Berlin, Germany: Springer.
14. Blickhan R. 1989 The spring-mass model for running and hopping. *J Biomech* **22**, 1217–1227. (doi:10.1016/0021-9290(89)90224-8)
15. McMahon TA, Cheng GC. 1990 The mechanics of running: how does stiffness couple with speed? *J. Biomech.* **23**(Suppl. 1), 65–78. (doi:10.1016/0021-9290(90)90042-2)
16. Abourachid A, Hackert R, Herbin M, Libourel PA, Lambert F, Gioanni H, Provini P, Blazevic P, Hugel V. 2011 Bird terrestrial locomotion as revealed by 3D kinematics. *Zoology* **114**, 360–368. (doi:10.1016/j.zool.2011.07.002)
17. Daley MA, Felix G, Biewener AA. 2007 Running stability is enhanced by a proximo-distal gradient in joint neuromechanical control. *J. Exp. Biol.* **210**, 383–394. (doi:10.1242/jeb.02668)
18. Muir GD, Gosline JM, Steeves JD. 1996 Ontogeny of bipedal locomotion: walking and running in the chick. *J. Physiol.* **493**, 589–601.
19. Roberts TJ, Chen MS, Taylor CR. 1998 Energetics of bipedal running. II. Limb design and running mechanics. *J. Exp. Biol.* **201**, 2753–2762.
20. Roberts TJ, Scales JA. 2002 Mechanical power output during running accelerations in wild turkeys. *J. Exp. Biol.* **205**, 1485–1494.
21. Maus HM, Lipfert SW, Gross M, Rummel J, Seyfarth A. 2010 Upright human gait did not provide a major mechanical challenge for our ancestors. *Nat. Commun.* **1**, 70. (doi:10.1038/ncomms1073)
22. Usherwood JR, Hubel TY. 2012 Energetically optimal running requires torques about the centre of mass. *J. R. Soc. Interface* **9**, 2011–2015. (doi:10.1098/rsif.2012.0145)
23. Daley MA, Biewener AA. 2003 Muscle force-length dynamics during level versus incline locomotion: a comparison of *in vivo* performance of two guinea fowl ankle extensors. *J. Exp. Biol.* **206**, 2941–2958. (doi:10.1242/jeb.00503)
24. Ahn AN, Furrow E, Biewener AA. 2004 Walking and running in the red-legged running frog, *Kassina maculata*. *J. Exp. Biol.* **207**, 399–410. (doi:10.1242/jeb.00761)
25. Blickhan R, Seyfarth A, Geyer H, Grimmer S, Wagner H, Gunther M. 2007 Intelligence by mechanics. *Phil. Trans. R. Soc. A* **365**, 199–220. (doi:10.1098/rsta.2006.1911)
26. Verstappen M, Aerts P. 2000 Terrestrial locomotion in the black-billed magpie. I. Spatio-temporal gait characteristics. *Motor Control* **4**, 150–164.
27. Verstappen M, Aerts P, Van Damme R. 2000 Terrestrial locomotion in the black-billed magpie: kinematic analysis of walking, running and out-of-phase hopping. *J. Exp. Biol.* **203**, 2159–2170.
28. Gatesy SM. 1990 Caudefemoral musculature and the evolution of theropod locomotion. *Paleobiology* **16**, 170–186.
29. Farris DJ, Sawicki GS. 2012 Human medial gastrocnemius force–velocity behavior shifts with locomotion speed and gait. *Proc. Natl Acad. Sci. USA* **109**, 977–982. (doi:10.1073/pnas.1107972109)
30. Roberts TJ, Marsh RL, Weyand PG, Taylor CR. 1997 Muscular force in running turkeys: the economy of minimizing work. *Science* **275**, 1113–1115. (doi:10.1126/science.275.5303.1113)
31. Full RJ, Koditschek DE. 1999 Templates and anchors: neuromechanical hypotheses of legged locomotion on land. *J. Exp. Biol.* **202**, 3325–3332.
32. Lipfert SW, Günther M, Renjewski D, Grimmer S, Seyfarth A. 2012 A model-experiment comparison of system dynamics for human walking and running. *J. Theor. Biol.* **292**, 11–17. (doi:10.1016/j.jtbi.2011.09.021)
33. Katz B. 1939 The relation between force and speed in muscular contraction. *J. Physiol.* **96**, 45–64.
34. Edman KA, Elzinga G, Noble MI. 1978 Enhancement of mechanical performance by stretch during tetanic contractions of vertebrate skeletal muscle fibres. *J. Physiol.* **281**, 139–155.
35. Fischer MS, Blickhan R. 2006 The tri-segmented limbs of therian mammals: kinematics, dynamics, and self-stabilization: a review. *J. Exp. Zool.* **305**, 935–952. (doi:10.1002/jez.a.333)
36. Fischer MS, Schilling N, Schmidt M, Haarhaus D, Witte H. 2002 Basic limb kinematics of small therian mammals. *J. Exp. Biol.* **205**, 1315–1338.
37. Andrada E, Mämpel J, Schmidt A, Fischer MS, Witte H. 2013 From biomechanics of rats' inclined locomotion to a climbing robot. *Int. J. Des. Nat. Ecodyn.* **8**, 191–212. (doi:10.2495/DNE-V8-N3-192-212)
38. Reilly SM, McElroy EJ, Biknevicius AR. 2007 Posture, gait and the ecological relevance of locomotor costs and energy-saving mechanisms in tetrapods. *Zoology* **110**, 271–289. (doi:10.1016/j.zool.2007.01.003)
39. Hancock JA, Stevens NA, Biknevicius AR. 2007 Whole-body mechanics and kinematics of terrestrial locomotion in the elegant-crested tinamou *Eudromia elegans*. *Ibis* **149**, 605–614. (doi:10.1111/j.1474-919X.2007.00688.x)
40. Nyakatura JA, Andrada E. 2014 On vision in birds: coordination of head-bobbing and gait stabilises vertical head position in quail. *Front. Zool.* **11**, 27. (doi:10.1186/1742-9994-11-27)
41. Stoessel A, Kilbourne BM, Fischer MS. 2013 Morphological integration versus ecological plasticity in the avian pelvic limb skeleton. *J. Morphol.* **274**, 483–495. (doi:10.1002/jmor.20109)
42. Muller R, Blickhan R. 2010 Running on uneven ground: leg adjustments to altered ground level. *Hum. Mov. Sci.* **29**, 578–589. (doi:10.1016/j.humov.2010.04.007)
43. Cavagna G. 2006 The landing–take-off asymmetry in human running. *J. Exp. Biol.* **209**, 4051–4060. (doi:10.1242/jeb.02344)
44. Maykranz D, Seyfarth A. 2014 Compliant ankle function results in landing-take off asymmetry in legged locomotion. *J. Theor. Biol.* **349**, 44–49. (doi:10.1016/j.jtbi.2014.01.029)
45. Clark KP, Ryan LJ, Weyand PG. 2014 Foot speed, foot-strike and footwear: linking gait mechanics and running ground reaction forces. *J. Exp. Biol.* **217**, 2037–2040. (doi:10.1242/jeb.099523)
46. Weyand PG, Sternlight DB, Bellizzi MJ, Wright S. 2000 Faster top running speeds are achieved with greater ground forces not more rapid leg movements. *J. Appl. Physiol.* **89**, 1991–1999.
47. Geyer H, Seyfarth A, Blickhan R. 2006 Compliant leg behaviour explains basic dynamics of walking and running. *Proc. R. Soc. B* **273**, 2861–2867. (doi:10.1098/rspb.2006.3637)
48. Seipel J, Holmes P. 2007 A simple model for clock-actuated legged locomotion. *Regul. Chaotic Dyn.* **12**, 502–520. (doi:10.1134/S1560354707050048)
49. Ankarali MM, Saranli U. 2010 Stride-to-stride energy regulation for robust self-stability of a torque-actuated dissipative spring-mass hopper. *Chaos* **20**, 033121. (doi:10.1063/1.3486803)
50. Shen ZH, Seipel JE. 2012 A fundamental mechanism of legged locomotion with hip torque and leg damping. *Bioinspir. Biomim.* **7**, 046010. (doi:10.1088/1748-3182/7/4/046010)
51. Farley CT, Houdijk HHP, Van Strien C, Louie M. 1998 Mechanism of leg stiffness adjustment for hopping on surfaces of different stiffnesses. *J. Appl. Physiol.* **85**, 1044–1055.
52. Grimmer S, Ernst M, Günther M, Blickhan R. 2008 Running on uneven ground: leg adjustment to vertical steps and self-stability. *J. Exp. Biol.* **211**, 2989–3000. (doi:10.1242/jeb.014357)
53. Müller R, Ernst M, Blickhan R. 2012 Leg adjustments during running across visible and camouflaged incidental changes in ground level. *J. Exp. Biol.* **215**, 3072–3079. (doi:10.1242/jeb.072314)
54. Birn-Jeffery AV, Daley MA. 2012 Birds achieve high robustness in uneven terrain through active control of landing conditions. *J. Exp. Biol.* **215**, 2117–2127. (doi:10.1242/jeb.065557)
55. Daley MA, Usherwood JR, Felix G, Biewener AA. 2006 Running over rough terrain: guinea fowl maintain dynamic stability despite a large unexpected change in substrate height. *J. Exp. Biol.* **209**, 171–187. (doi:10.1242/jeb.01986)
56. Hutchinson JR, Allen V. 2009 The evolutionary continuum of limb function from early theropods to birds. *Die Naturwissenschaften* **96**, 423–448. (doi:10.1007/s00114-008-0488-3)